Black Holes

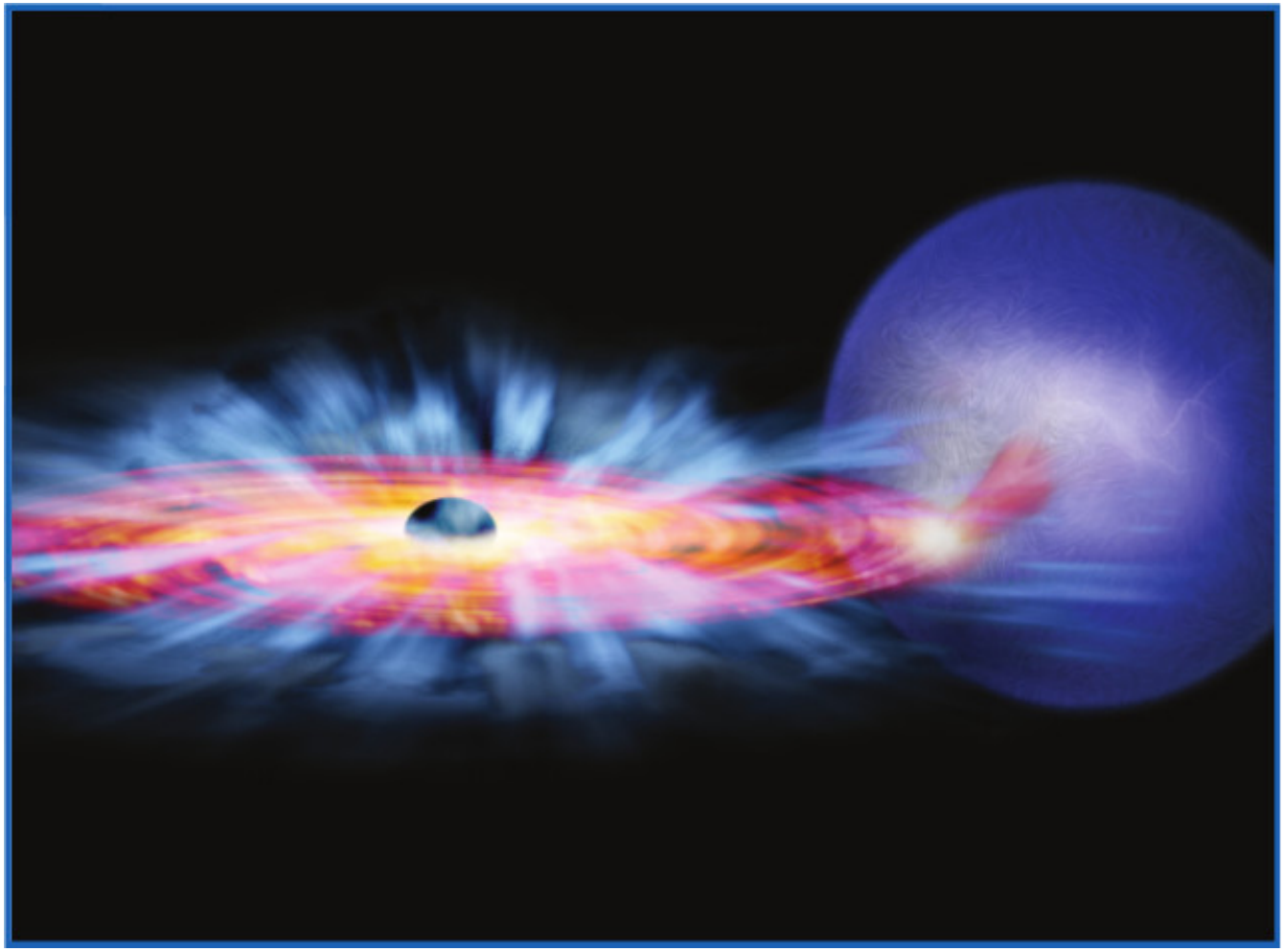

Black Hole and Host Galaxy Mass Estimates

1. Constraining the mass of a BH in a spectroscopic binary.

2. Constraining the mass of a supermassive BH from reverberation mapping and emission line widths.

3. Estimating the mass of a supermassive BH from the virial theorem.

4. Estimating the mass of a supermassive BH from the M-σ relation.

5. Constraining the mass of the host Galaxy from gravitational lensing.

Black-Hole Mass Estimates in Spectroscopic Binaries

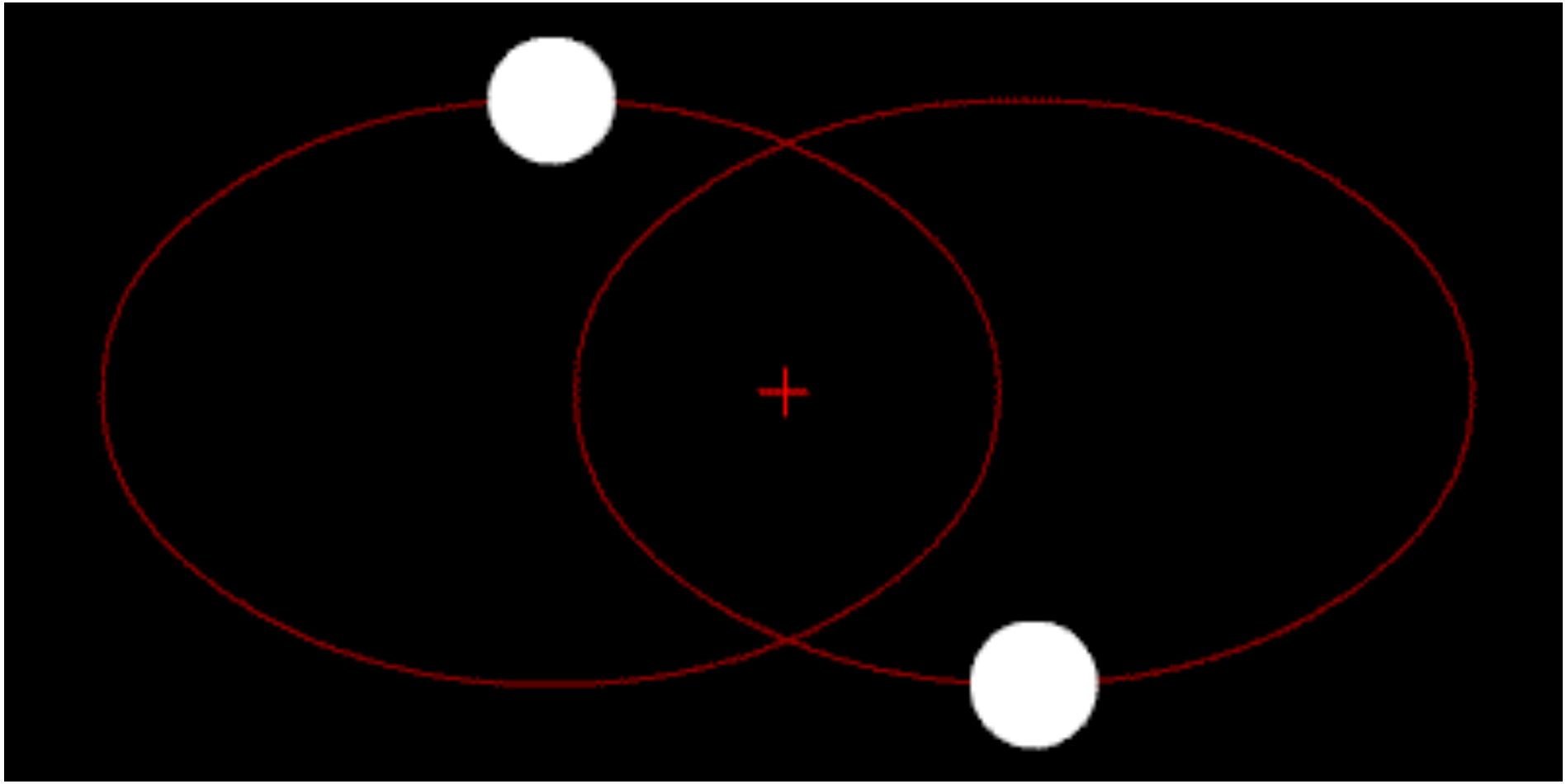

Double Stars

Double star: A pair of stars located at nearly the same position in the night sky. Some, but not all, double stars orbit each other.

Optical double star: **Two stars** that lie along nearly the same line of sight but are actually **at very different distances from us**.

Binary stars: Two stars orbiting about each other. The brighter star is called the primary and the other is its companion star or secondary. A double star can be either an optical double of a binary star.

Visual Binary: a binary star for which the **angular separation between the two components is great** enough to permit them to be observed as pair of stars.

Binary Stars

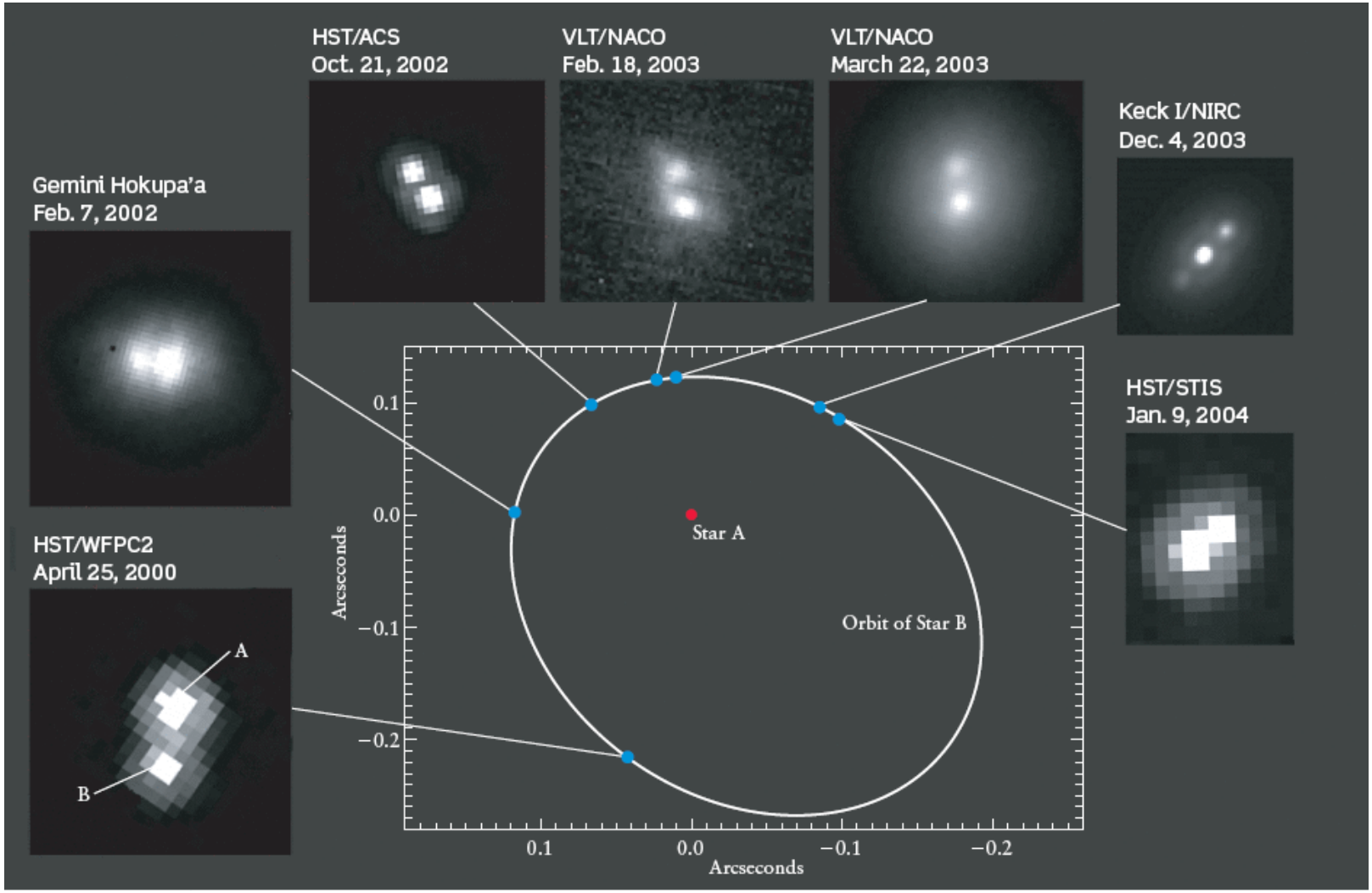

Binary Star 2MASSW J0746425 +2000321

Spectroscopic Binaries

One can also use the Doppler effect to determine if a star is a binary.

If the spectrum contains absorption lines that periodically shift in wavelength one can infer that they are looking at more that one star.

spectroscopic binary: A binary star system whose binary nature is deduced from the periodic Doppler shifting of lines in its spectrum.

If the spectrum of only one star of the binary is detectable it is called a **single-line spectroscopic binary**.

Spectroscopic Binaries

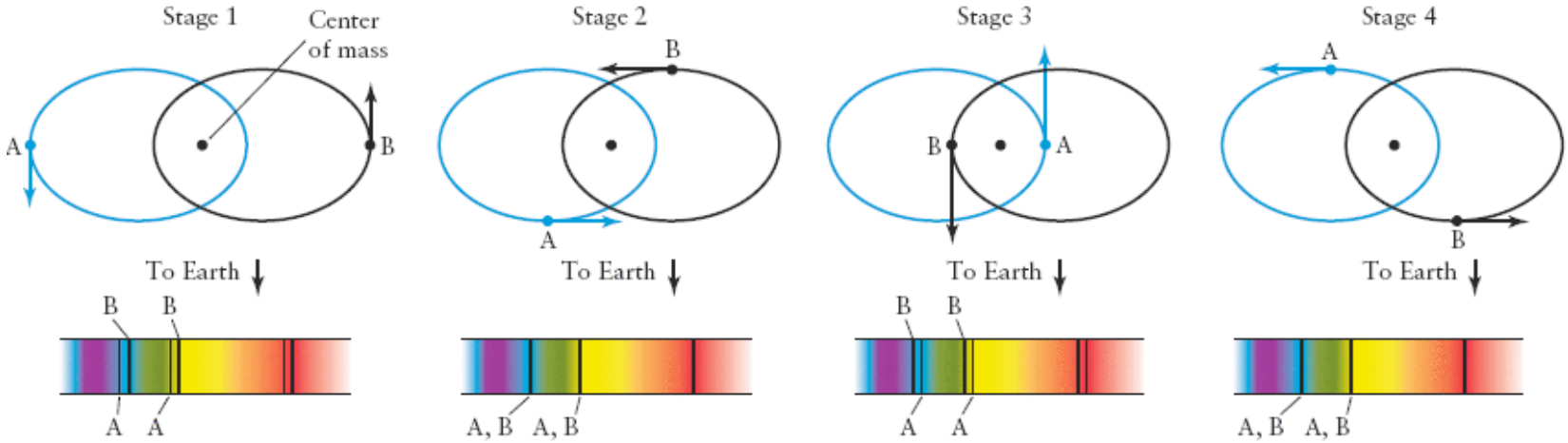

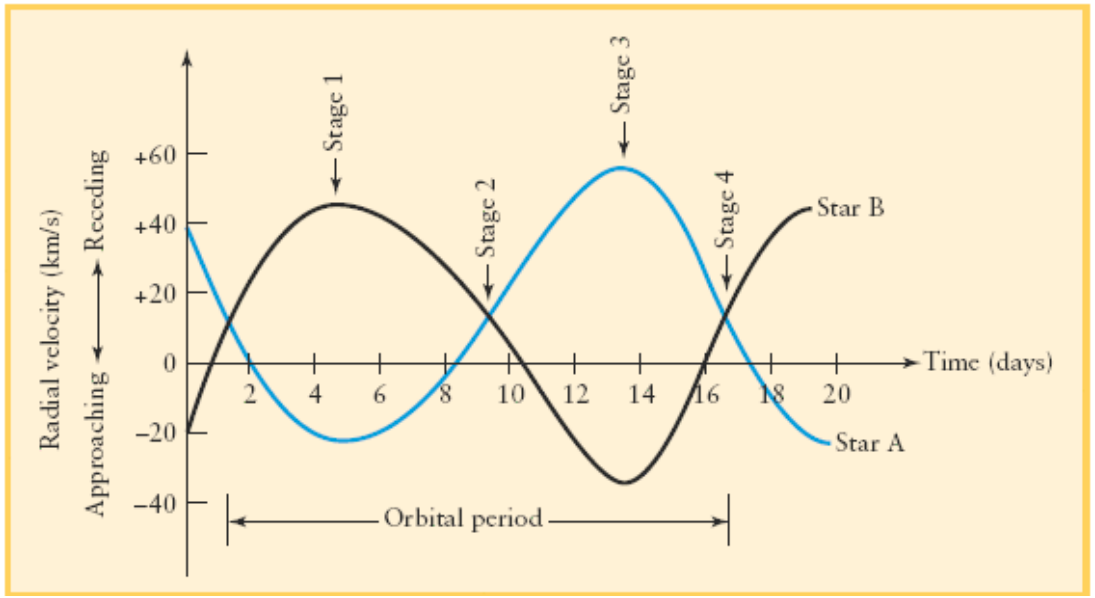

Radial Velocity Curves of Spectroscopic binary system HD 171978

Spectroscopic Binaries

Assumptions and definitions:
The angle between the true orbital plane and the observed one is called the inclination angle *i*. For simplicity we assume circular orbits ($e = 0$).

v_1, v_2 are the velocities of the objects with masses m_1,m_2 respectively.

The inferred radial velocities (via Doppler shift) are:

$$v_{1r} = v_1 \sin i, \quad v_{2r} = v_2 \sin i$$

$$v_1 = 2\pi a_1/P, \; v_2 = 2\pi a_2/P$$

Where a_1, a_2 are the radii (semimajor axes) of the orbits and P is the period of the binary.

Spectroscopic Binaries

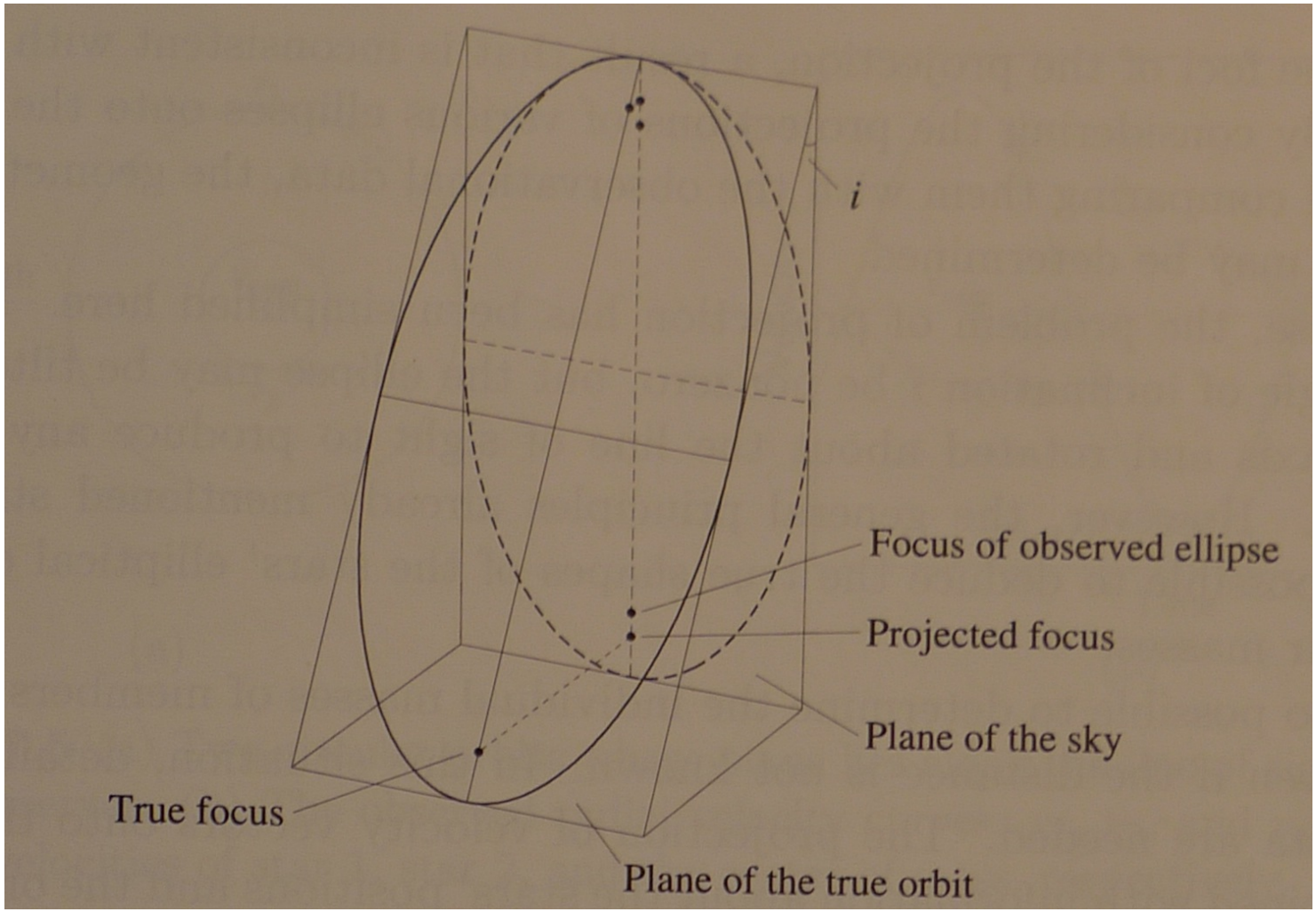

An elliptical orbit projected onto the plane of the sky produces an observable elliptical orbit. The foci of the original orbit do not project onto the foci of the projected ellipse.

Spectroscopic Binaries

We take the center of mass as the center of our coordinate system. $R_{cm} = (m_1a_1 - m_2a_2)/(m_1+m_2) = 0$
Conservation of momentum gives: $m_1v_1 = m_2v_2$

$$\frac{m_1}{m_2} = \frac{v_2}{v_1} = \frac{v_2 sini}{v_1 sini} = \frac{v_{2r}}{v_{1r}}$$

$$a = a_1 + a_2 = \frac{P}{2\pi}(v_1 + v_2)$$

Keppler's Modified 3rd Law:

$$P^2 = \frac{4\pi^2}{G}\frac{a^3}{(m_1 + m_2)}$$

Spectroscopic Binaries

$$(m_1 + m_2) = \frac{P}{2\pi G}\frac{(v_{1r}+v_{2r})^3}{sin^3 i} \Longrightarrow$$

$$\frac{m_2^3}{(m_1+m_2)^2} sin^3 i = \frac{P v_{1r}^3}{2\pi G} : \textit{mass function}$$

The mass function only depends on observable quantities and places a lower limit on the mass m_2 (ie $m_2 > f(m)$)

Masses of Neutron Stars and Black Holes in Binaries

The diagram shows masses of the compact objects in binaries as estimated using Kepler's modified 3rd law.

The compact objects left of the vertical dashed line are thought to be neutron stars and those to the right black holes.

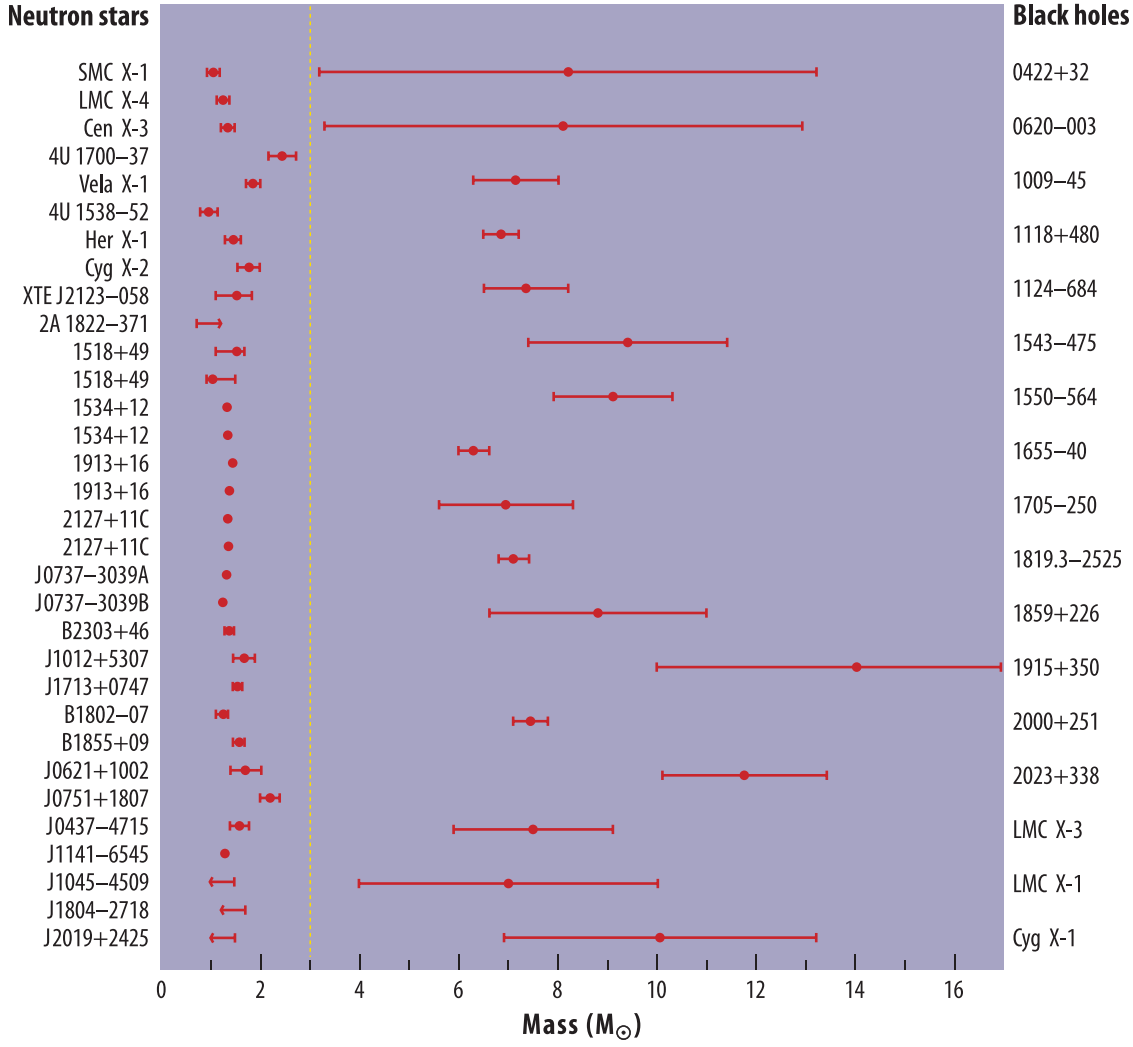

Determining BH Masses in AGN

Direct methods of measuring BH masses in AGN using stellar dynamics requires high spatial resolution and is limited to nearby galaxies.

A promising method relies on **reverberation mapping** of broad emission lines.

Reverberation mapping is based on measuring the time lag between variations in the flux from a central source of ionizing radiation and the response of the emission lines from photoionized gas in the broad line region. Blandford & McKee 1982, Peterson 1993, Netzer & Peterson 1997)

AGN Paradigm

Narrow line gas:
Low density ionized gas with $n_e \sim 10^3$-$10^6 cm^{-3}$ producing forbidden narrow lines with widths of ~ 100 km/s

Broad line gas:
High density ionized gas with $n_e > 10^9$ cm^{-3} producing permitted lines with widths of up to 10^4 km/s

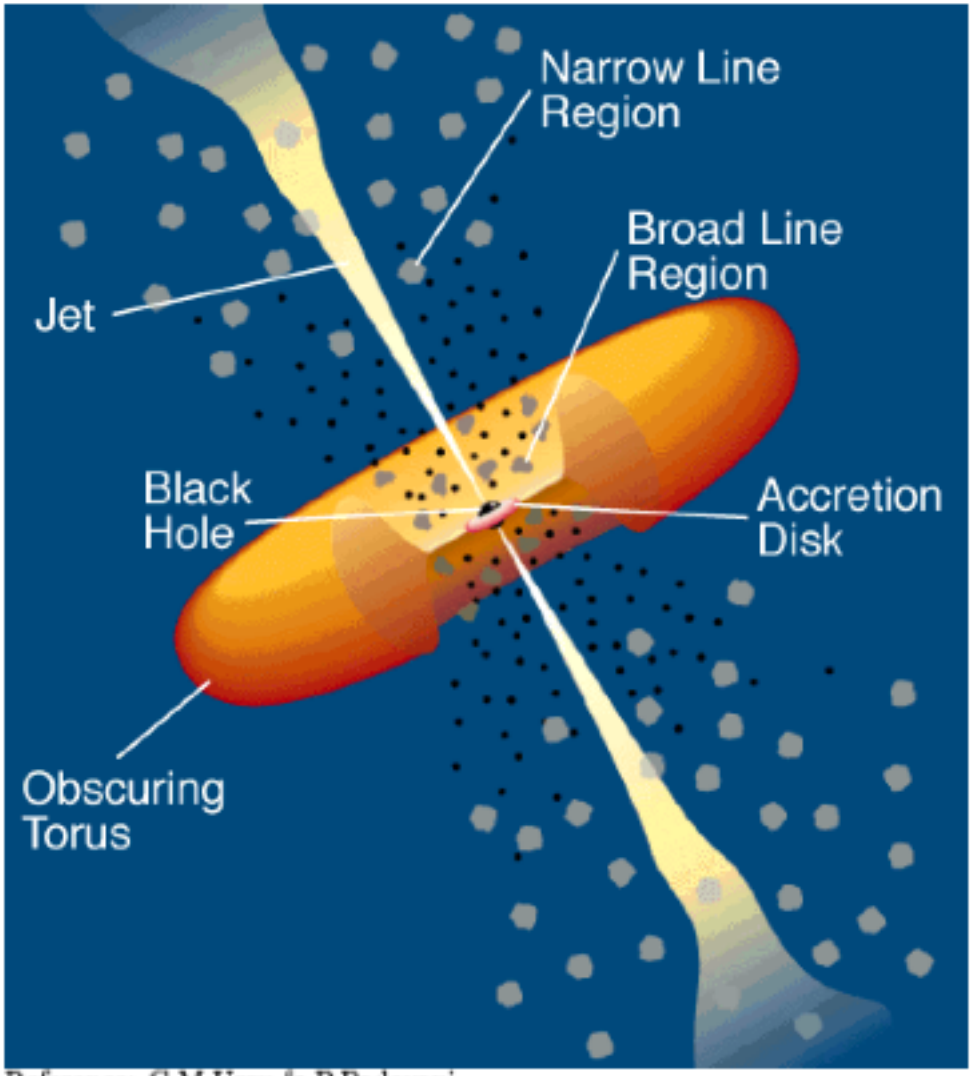

Reference: C.M.Urry & P.Padovani

AGN

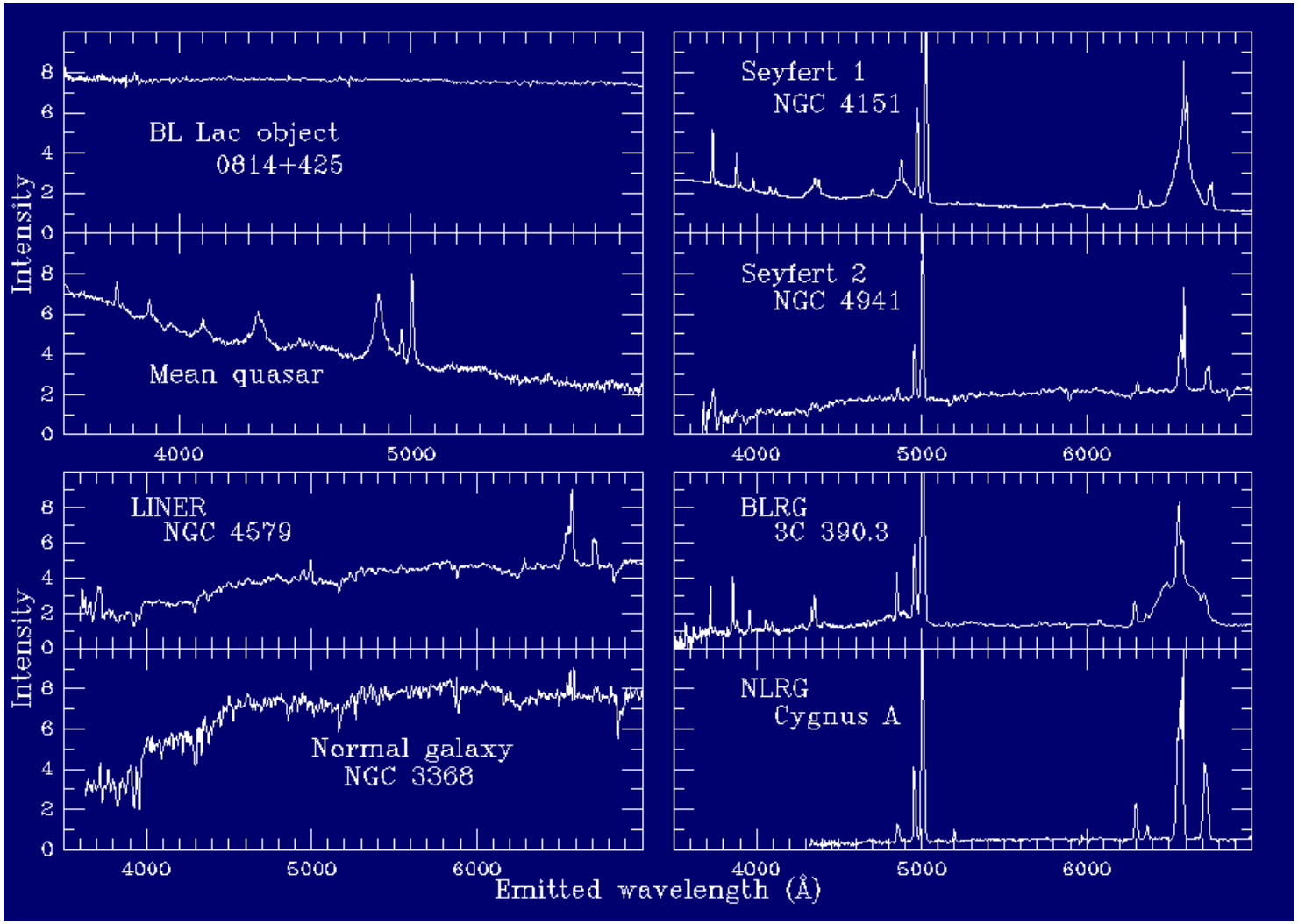

The distinctions among various flavors of AGN rely on spectroscopic clues.

Determining BH Masses in AGN

The BH mass in an AGN is given by the virial equation:

$$M_{BH} \approx \frac{f R \Delta v^2}{G}$$

where Δv is the width of the broad emission line H_β , R is the distance of the broad line clouds from the BH and *f* is a scale factor ~ 1 that depends on the BLR geometry.

Observations show that $R \propto L^\gamma$, where *L* is the AGN's continuum luminosity. The AGNs luminosity can therefore be used as a surrogate for *R* in the M_{BH} equation.

The mass scaling relationships for obtaining BH masses of AGN are (Vestergaard and Peterson, 2006, ApJ, 641, 68) :

1. FWHM(Hβ) and L_λ(5100 Å): For the optical continuum luminosity and FWHM of the Hβ broad component,

$$\log M_{\rm BH}({\rm H}\beta) = \log\left\{ \left[\frac{{\rm FWHM(H}\beta)}{1000\ {\rm km\ s^{-1}}}\right]^2 \left[\frac{\lambda L_\lambda(5100\ {\rm Å})}{10^{44}\ {\rm ergs\ s^{-1}}}\right]^{0.50} \right\} + (6.91 \pm 0.02). \quad (5)$$

The sample standard deviation of the weighted average zero-point offset, which shows the intrinsic scatter in the sample, is $\pm$0.43 dex. This value is more representative of the uncertainty in the zero point than is the formal error.

2. FWHM(Hβ) and L(Hβ): For the Hβ broad-line component luminosity and FWHM,

$$\log M_{\rm BH}({\rm H}\beta) = \log\left\{ \left[\frac{{\rm FWHM(H}\beta)}{1000\ {\rm km\ s^{-1}}}\right]^2 \left[\frac{L({\rm H}\beta)}{10^{42}\ {\rm ergs\ s^{-1}}}\right]^{0.63} \right\} + (6.67 \pm 0.03). \quad (6)$$

$\lambda_{H\beta} = 486.1$ nm

The mass scaling relationships for obtaining BH masses of AGN are (Vestergaard and Peterson, 2006, ApJ, 641, 68) :

3. FWHM(C IV) and L_λ(1350 Å): For the ultraviolet continuum luminosity and the FWHM of the C IV line,

$$\log M_{\rm BH}({\rm C\ IV}) = \log\left\{\left[\frac{{\rm FWHM(C\ IV)}}{1000\ {\rm km\ s^{-1}}}\right]^2\left[\frac{\lambda L_\lambda(1350\ {\rm Å})}{10^{44}\ {\rm ergs\ s^{-1}}}\right]^{0.53}\right\} + (6.66 \pm 0.01). \quad (7)$$

The sample standard deviation of the weighted average zero-point offset is ±0.36 dex.

4. σ_l(C IV) and L_λ(1350 Å): For the ultraviolet continuum luminosity and the dispersion of the C IV emission line,

$$\log M_{\rm BH}({\rm C\ IV}) = \log\left\{\left[\frac{\sigma_l({\rm C\ IV})}{1000\ {\rm km\ s^{-1}}}\right]^2\left[\frac{\lambda L_\lambda(1350\ {\rm Å})}{10^{44}\ {\rm ergs\ s^{-1}}}\right]^{0.53}\right\} + (6.73 \pm 0.01). \quad (8)$$

The sample standard deviation of the weighted average zero-point offset is ±0.33 dex.

$\lambda_{\rm CIV} = 154.9$ nm

How Accurate is the single-epoch BH mass estimate?

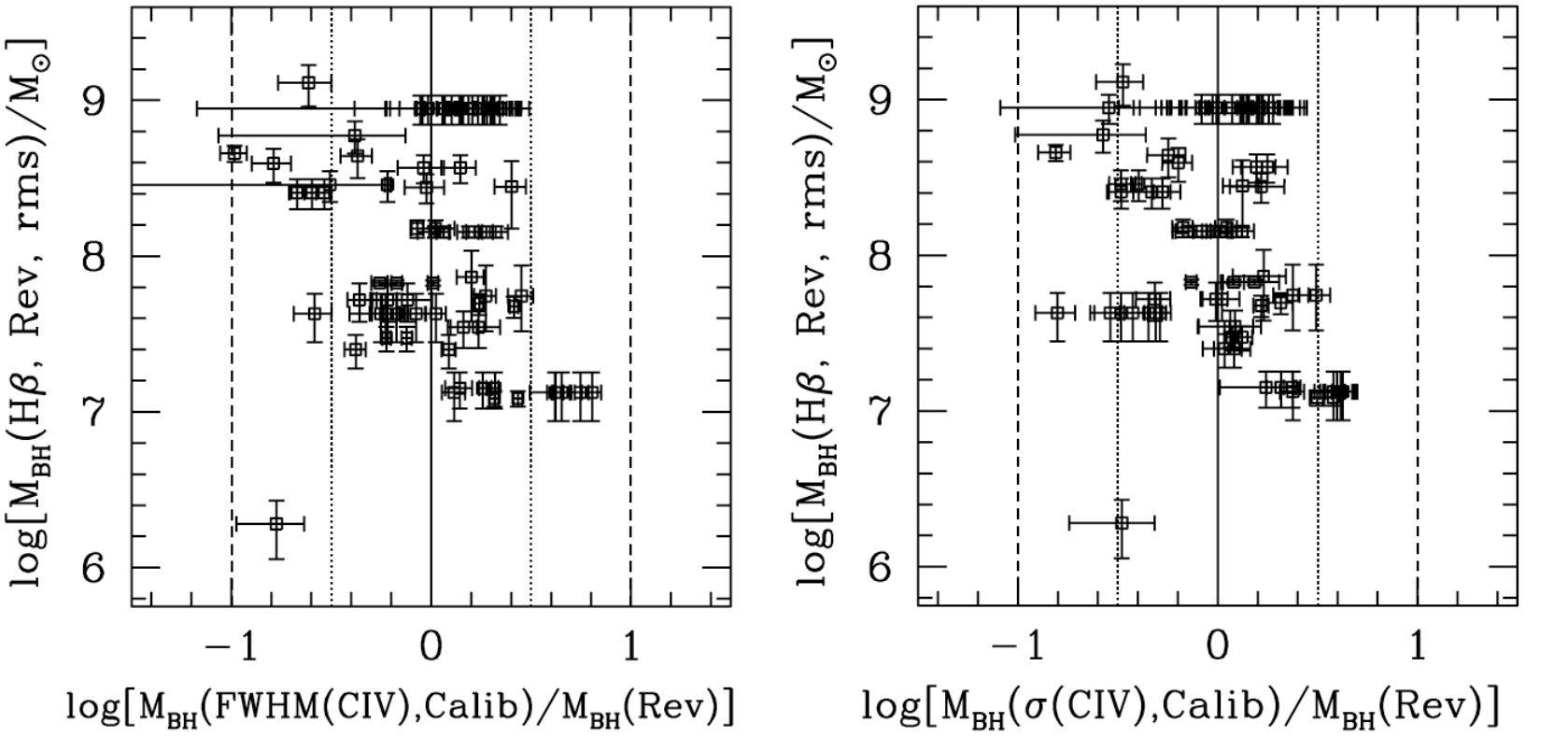

FIG. 9.—Deviation of the UV single-epoch black hole mass estimates from the reverberation mapping established mass $M_{\rm BH}$(Rev) plotted vs. $M_{\rm BH}$(Rev). *Left*: Single-epoch mass estimates based on FWHM(C IV) and L_λ(1350 Å). *Right*: Single-epoch mass estimates based on the line dispersion σ_l(C IV) and L_λ(1350 Å). The uncertainties in the abscissa are the (propagated) uncertainties in the single-epoch mass estimates (i.e., *not* the error in the mass deviation). A strictly unity relationship is indicated by the solid line. Offsets of ±0.5 and ±1 dex are indicated by the dotted and dashed lines, respectively. [*See the electronic edition of the Journal for a color version of this figure*.]

Estimate the mass of the SMBH in a Galaxy

Virial theorem: -2<K> = <U>

$$K = \sum_{1}^{N} \frac{1}{2} m_i v_i^2$$

$$U = \sum_{1}^{N} u_i$$

$-2\frac{1}{2} m \sum_1^N v_i^2 = \mathrm{U} \Longrightarrow -m\langle v^2 \rangle = \frac{U}{N}$ (1)

$\langle v^2 \rangle = \langle v_r^2 \rangle + \langle v_\vartheta^2 \rangle + \langle v_\varphi^2 \rangle = 3\langle v_r^2 \rangle$ (2)

(1) $\wedge$ (2) $\Longrightarrow -m\ 3\langle v_r^2 \rangle = \frac{U}{N}$ (3)

Velocity Dispersion: $\sigma^2 = \frac{1}{N}\sum_1^N (v_i - \langle v \rangle)^2 = \frac{1}{N}\sum_1^N (v_i)^2 = \langle v^2 \rangle \Longrightarrow$
$\sigma_r^2 = \langle v_r^2 \rangle$ (4)

(3) $\wedge$ (4) $\Longrightarrow -3m\sigma_r^2 = \frac{U}{N}$ (5)

Estimate the mass of the SMBH in a Galaxy

Derivation of total potential energy of N stars of mass m that are uniformly distributed within a sphere of radius R

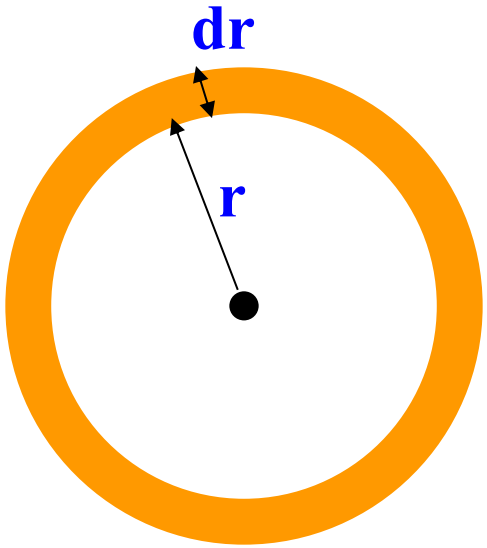

$$dU = -\frac{GM(<r)dm}{r}$$

$$M(<r) = \rho\frac{4}{3}\pi r^3$$

$$dm = 4\pi r^2 dr\rho$$

$$U = \int_0^R dU(r) = -\int_0^R G\frac{\rho\frac{4}{3}\pi r^3\, 4\pi r^2 dr\rho}{r} =$$

$$=G\frac{(4\pi)^2}{3}\rho^2\int_0^R r^4 dr \Longrightarrow U = -\frac{3}{5}\frac{GM^2}{R} \quad (6)$$

$$(5)\wedge(6) \Longrightarrow -3m\sigma_r^2 = -\frac{3}{5}\frac{GM^2}{RN} \Longrightarrow$$

$$M_{\text{Virial}} = \frac{5R\sigma_r^2}{G}$$

Estimate the mass of the SMBH in a Galaxy

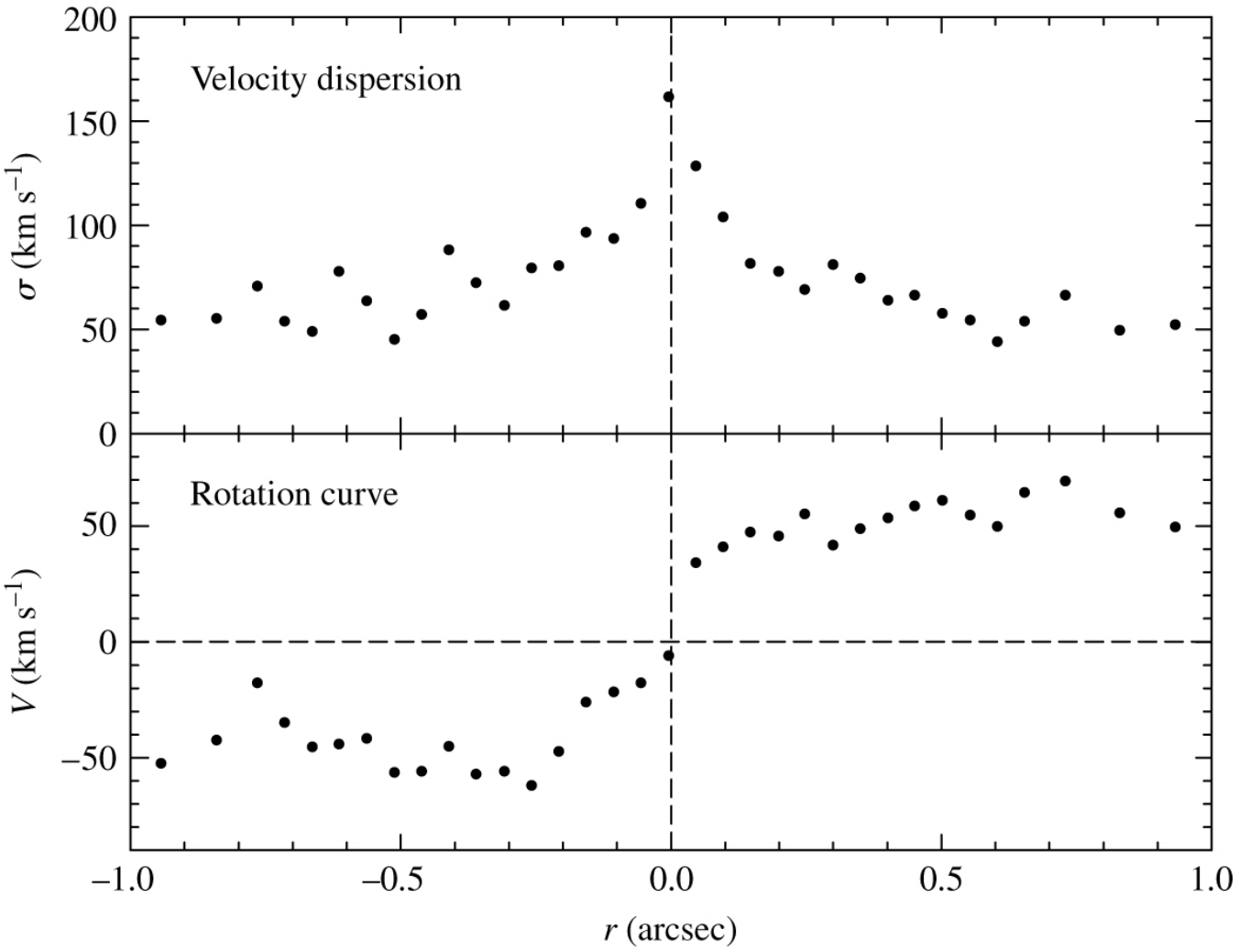

Black Hole Mass and Galaxy Bulge Mass

Observations in the 1990s had demonstrated a possible empirical **relationship between galaxy luminosity and black hole mass** but this relationship had large scatter (*Magorrian Relation)*.

The mean ratio of black hole mass to bulge mass is believed to be approximately 0.1% , i.e., a bulge of one billion solar masses contains a black hole of approximately one million solar masses.

Black Hole Mass – Velocity Dispersion Relation

The M_{BH}-σ relation is an empirical correlation between the stellar velocity dispersion σ of a galaxy bulge and the mass M of the supermassive black hole at the galaxy's center.

$$\sigma = \frac{1}{\sqrt{N}}\left[\sum_{1}^{N}\left(u - \langle u \rangle\right)^2\right]^{1/2}$$

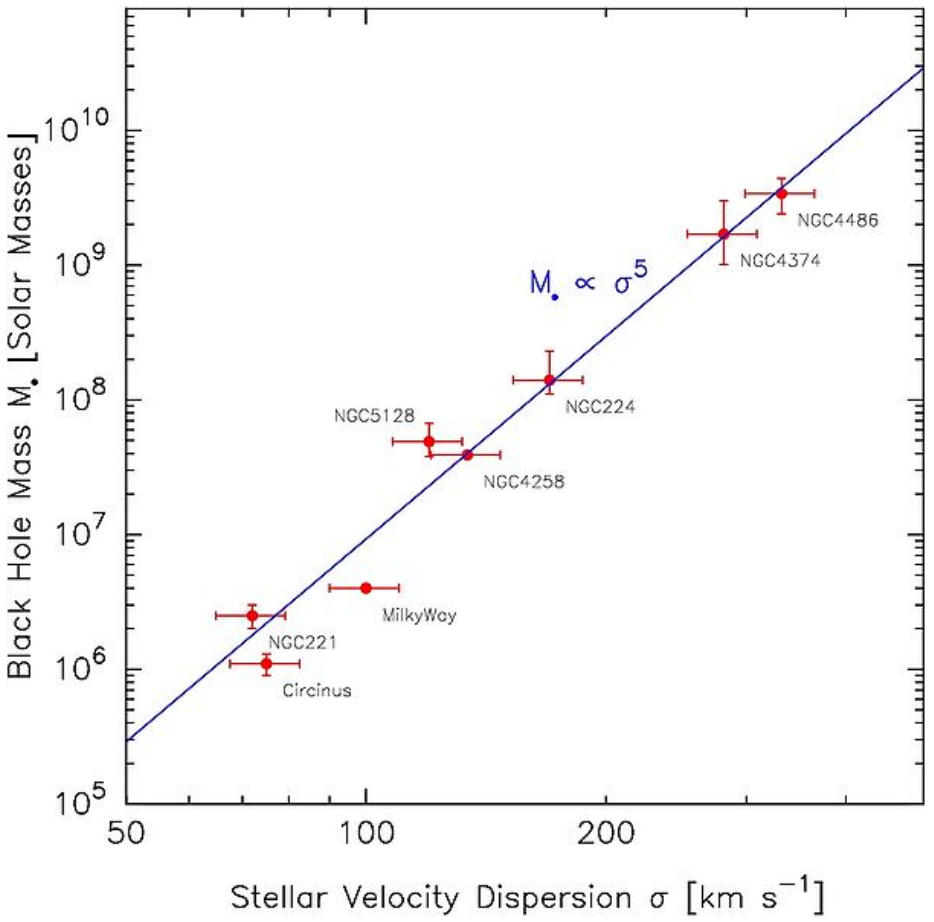

$$M_{BH} \propto \sigma^{\alpha},\ \alpha \approx 5$$

Macro and Microlensing of Quasars

Macrolensing is the bending of light produced by the global mass distribution of the lensing galaxy.

Microlensing is the bending of light produced by the individual stars in the lensing galaxy.

Microlensing variability occurs when the complex pattern of caustics produced by stars in the lens moves across the source plane.

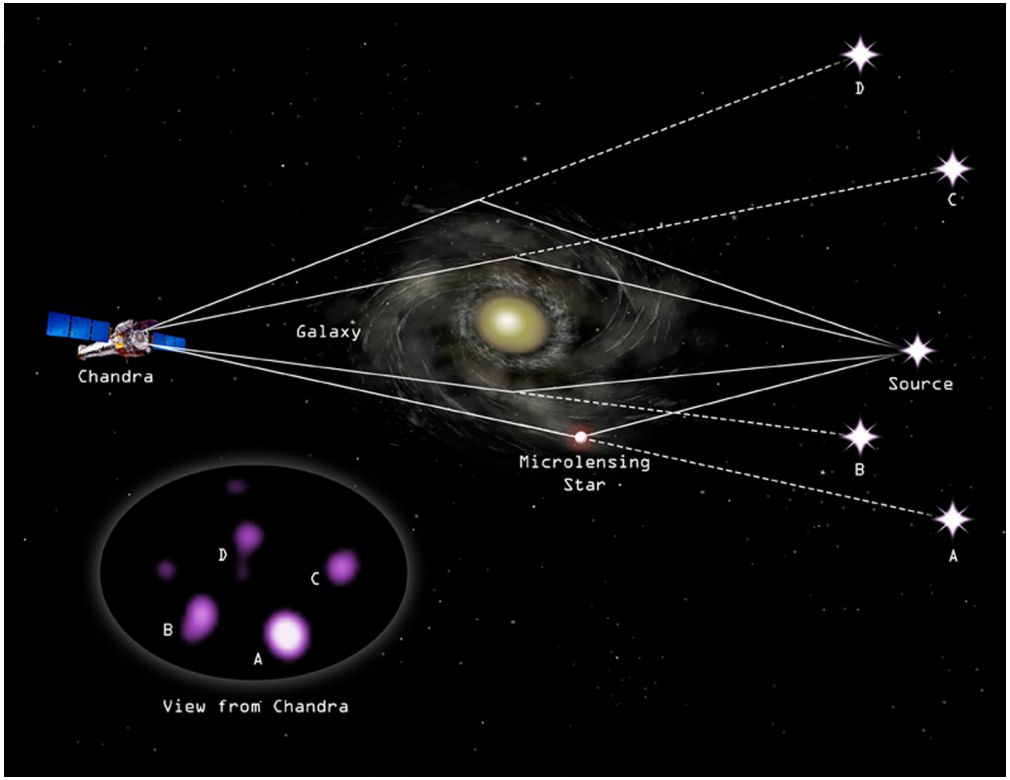

Conceptual diagram of the deflection of light in a 4-image gravitational lens system.

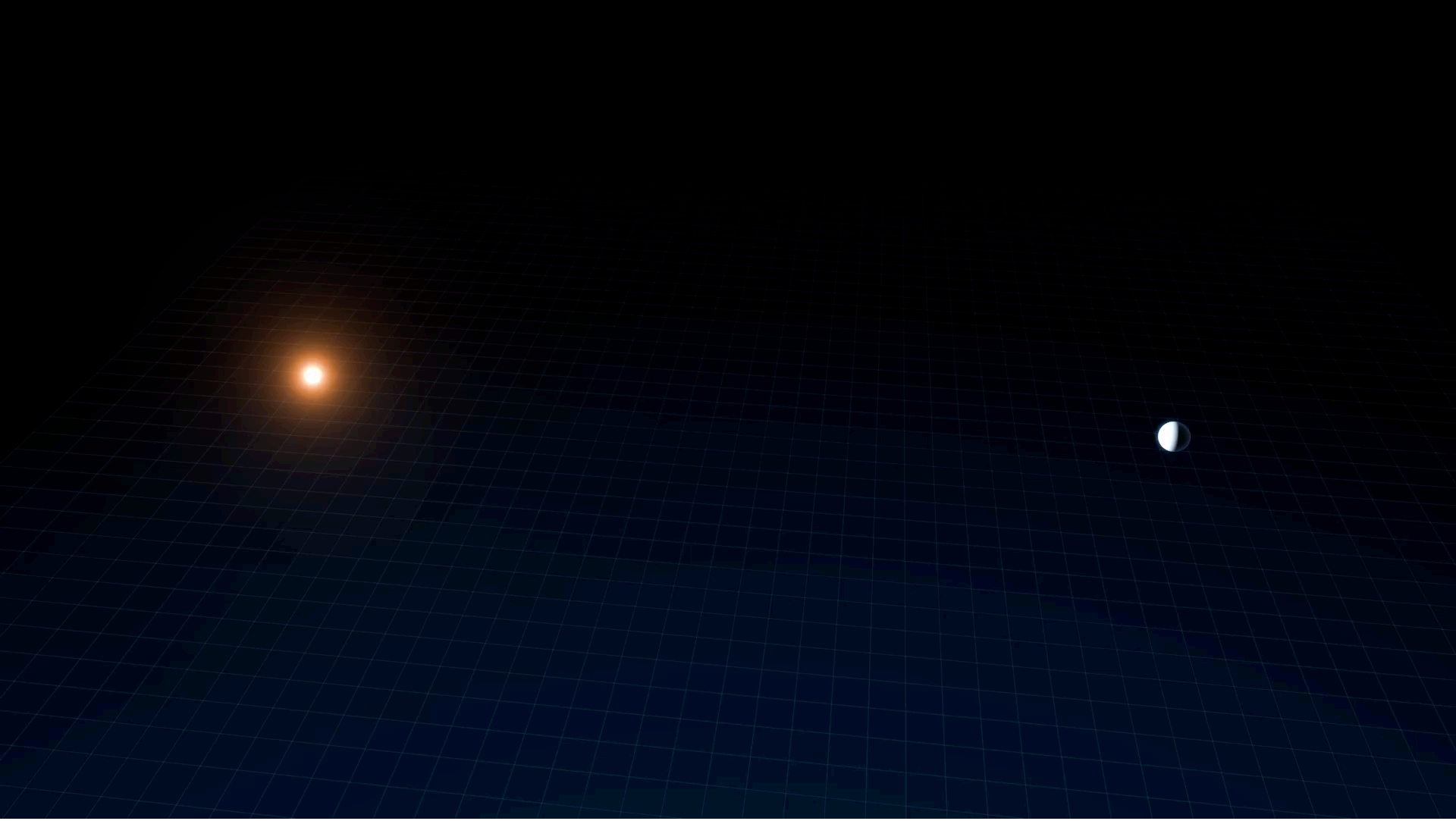

Gravitational Lensing; Basics

The two-dimensional lens equation is: $\vec{\beta} = \vec{\theta} - \vec{\alpha}(\vec{\theta})$

The reduced deflection angle is: $\vec{\alpha} = \frac{D_{LS}}{D_S}\tilde{\alpha}$

The position vector in the lens plane is: $\vec{\xi} = D_L\,\vec{\theta}$

The deflection angle at position ξ is the sum of the deflections due to all the mass elements in the lens plane:

$$\tilde{\alpha}(\vec{\xi}) = \frac{4G}{c^2}\int \frac{(\vec{\xi}-\vec{\xi'})\Sigma(\vec{\xi'})}{\left[\vec{\xi}-\vec{\xi'}\right]^2}\,d^2\xi'$$

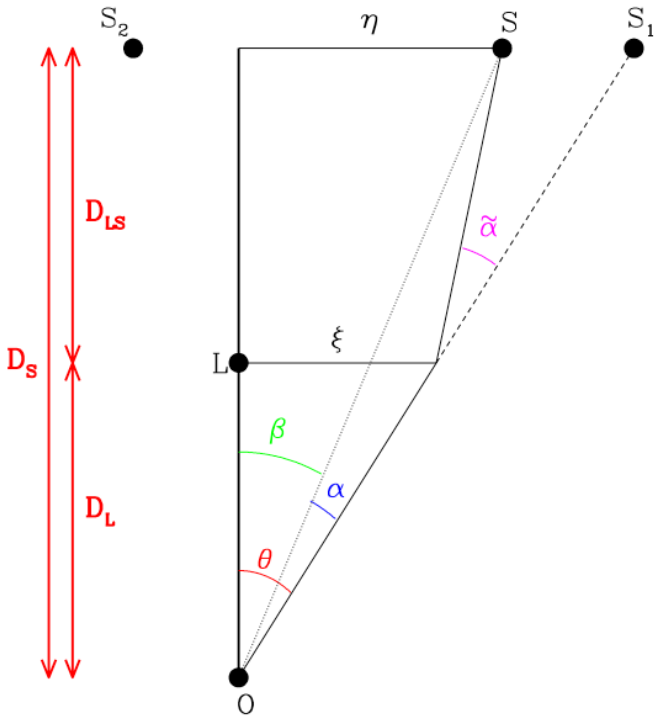

Gravitational Lensing; Basics

The deflection angle of a photon passing a distance ξ from a mass M is $a = 4GM/\xi c^2$ (in units of radians).

The lens equation from a point mass then becomes:

$$\theta^2 - \theta\beta - \frac{4GM}{c^2}\frac{D_{LS}}{D_L D_S} = 0$$

Solution:

$$\beta = \theta_1 + \theta_2 \quad \text{and M} = -\frac{\theta_1 \theta_2 c^2}{4G}\left(\frac{D_L D_S}{D_{LS}}\right)$$

Gravitational Lensing; Basics

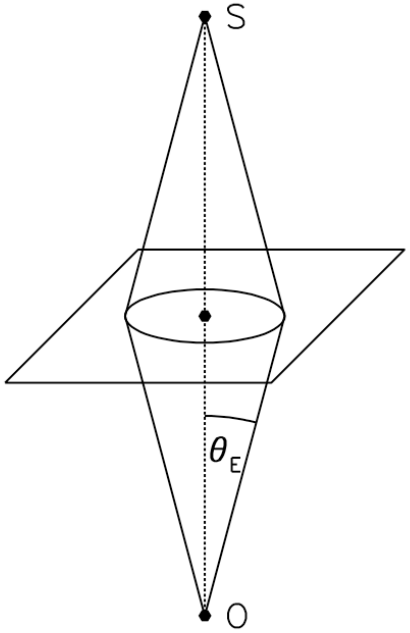

Several commonly used quantities in lensing are the critical surface-mass density, Σ_{crit} , and the the Einstein Radius, R_E.

Multiple images are produced when the surface mass density of the lens exceeds the critical value:

$$\Sigma_{crit} = \frac{c^2}{4\pi G}\frac{D_{LS}}{D_L D_S}$$

$\Sigma_{crit} \sim 0.8$ g cm^{-2} for lens and source redshifts of 0.5 and 2.0, respectively.

For the special case in which the source lies exactly behind the lens ($\beta = 0$) a ring-like image is produced with a radius (commonly referred to as the Einstein Radius) θ_E:

$$\theta_E = \sqrt{\frac{4\pi G}{c^2}\frac{D_{LS}}{D_L D_S}} = (0.9 arcsec)\left(\frac{M}{10^{11} M_\odot}\right)^{1/2}\left(\frac{D_L D_{LS}/D_S}{Gpc}\right)^{-1/2}$$

Gravitational Lensing; Basics

The magnification due to lensing of a point source obtains an infinite value at certain locations.

These locations are called **critical curves** in the lens plane (upper panel) and **caustics** in the source plane (lower panel). The numbers in the bottom panel identify regions in the source plane that correspond to 1,3 or 5 images, respectively.

Figure from J. Wambsganns, Gravitational Lensing in Astronomy, www.livingreviews.org/Articles/Volume1/1998-12wamb

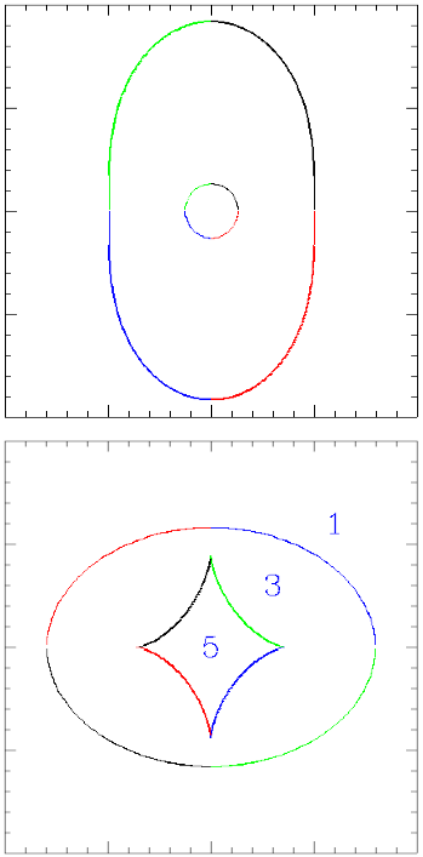

Gravitational Lensing; Basics

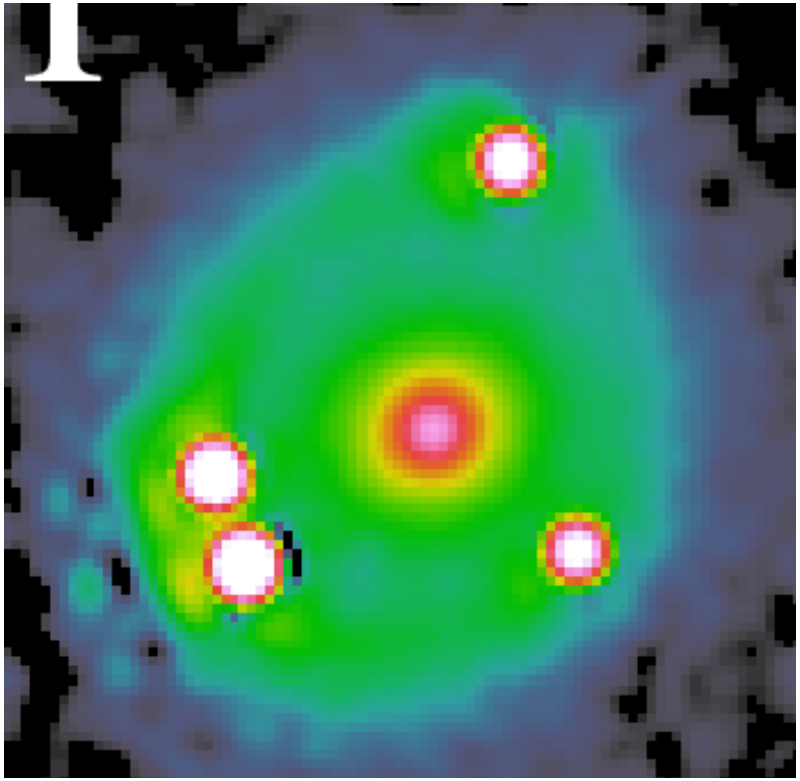

Hubble Space Telescope Image
of PG 1115+080 (H band)

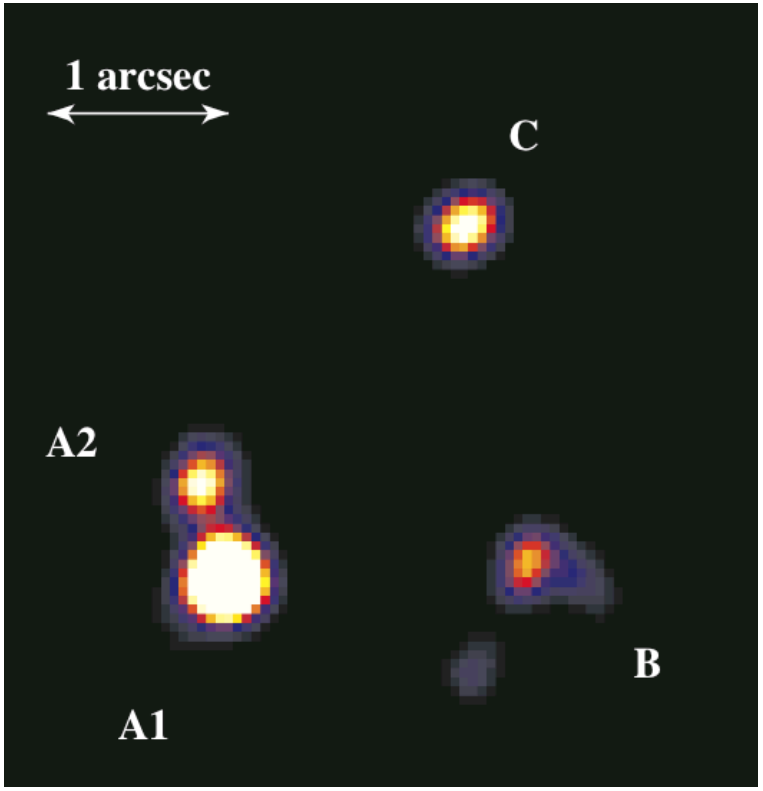

Chandra X-ray Observatory Image
of PG 1115+080 (deconvolved)

Microlensing; Basics

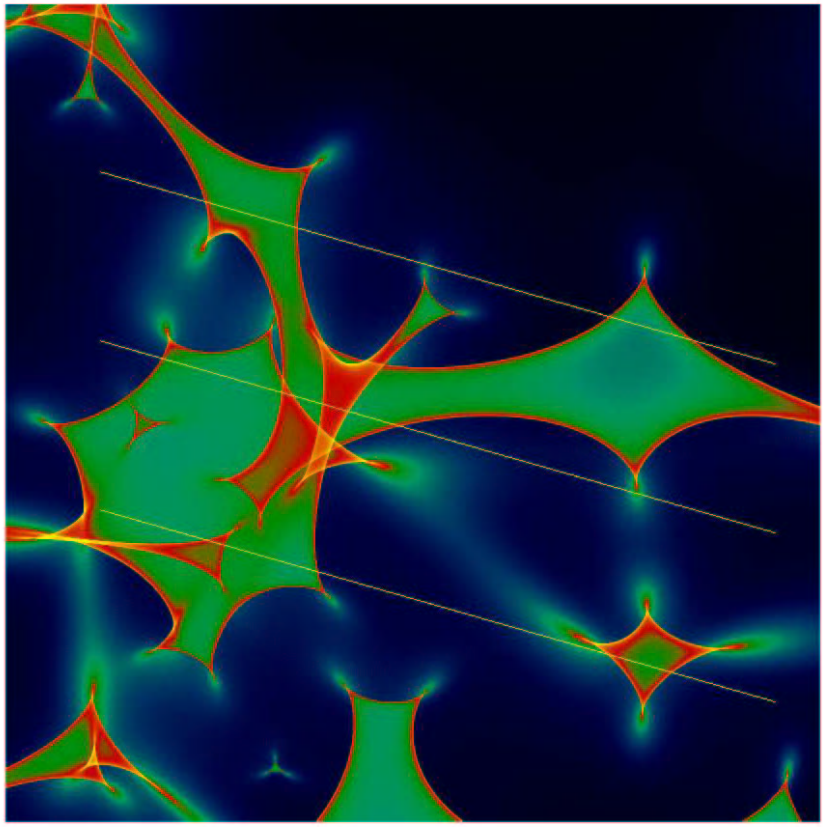

Figure 10: *Magnification pattern in the source plane, produced by a dense field of stars in the lensing galaxy. The color reflects the magnification as a function of the quasar position: the sequence blue-green-red-yellow indicates increasing magnification. Lightcurves taken along the yellow tracks are shown in Figure 11. The microlensing parameters were chosen according to a model for image A of the quadruple quasar Q2237+0305:* $\kappa = 0.36$, $\gamma = 0.44$.

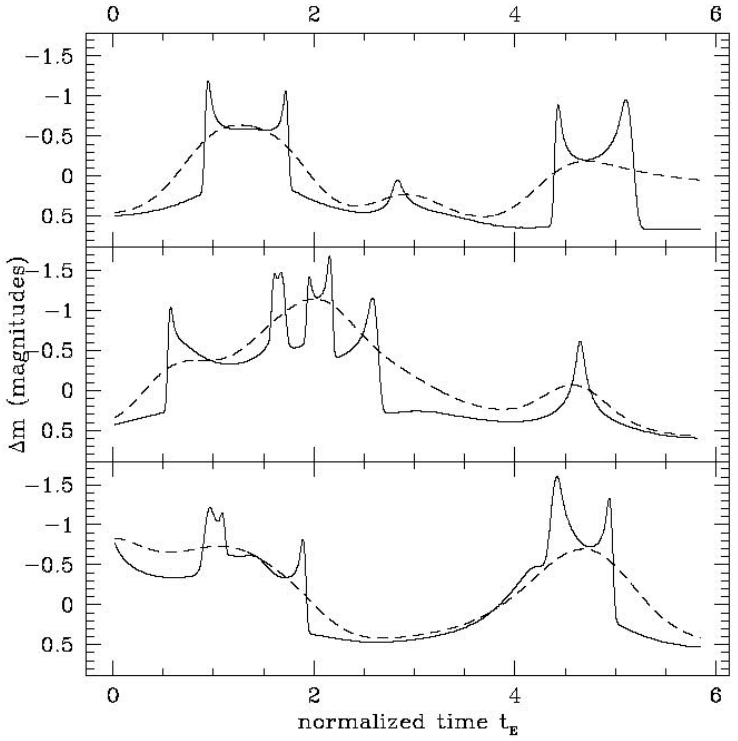

Figure 11: *Microlensing Lightcurve for the yellow tracks in Figure 10. The solid and dashed lines indicate relatively small and large quasar sizes. The time axis is in units of Einstein radii divided by unit velocity.*

Figures from J. Wambsganns, Gravitational Lensing in Astronomy, www.livingreviews.org/Articles/Volume1/1998-12wamb

Fiducial Model

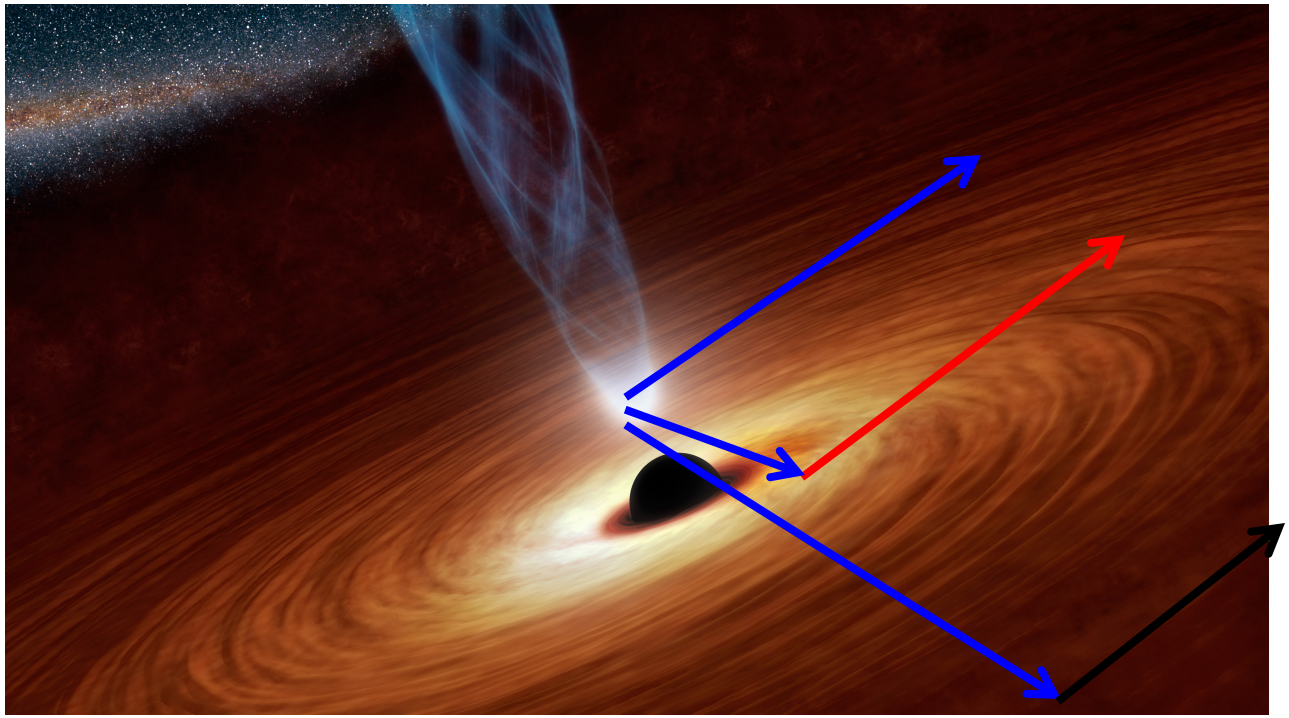

X-ray Power-Law from compact corona

Relativistically Blurred Reflection (line + continuum)

Distant Reflection (line + continuum)

Geometrically thin, optically thick accretion disk emitting primarily in UV/Optical

Incident and Reflected Accretion Disk Spectra

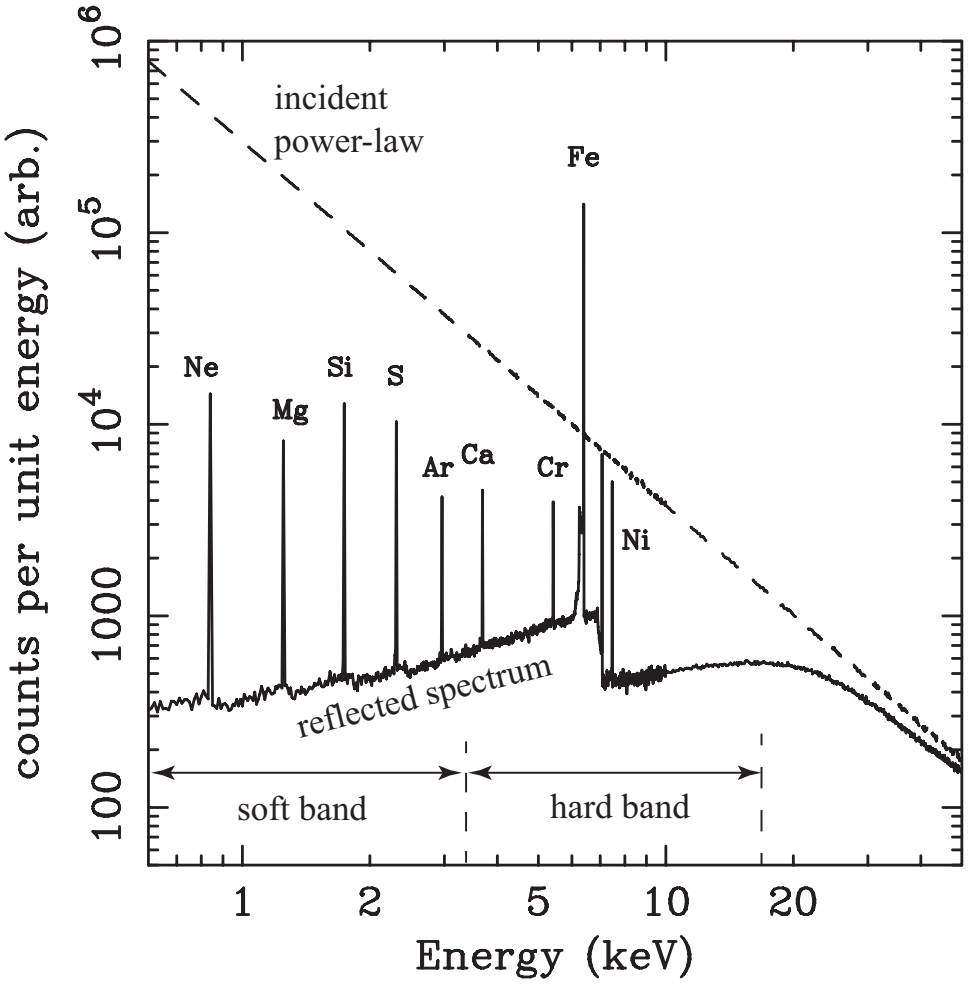

``Reflection'' of an incident power-law X-ray spectrum (dashed line) by a cold slab of gas with cosmic abundances. The principal observables from the reflection are the iron K fluorescent line at 6.40keV and a ``Compton reflection hump'' peaking at ~ 30 keV. Courtesy of Chris Reynolds.

Simulations of X-ray Microlensing in Quasar RXJ1131

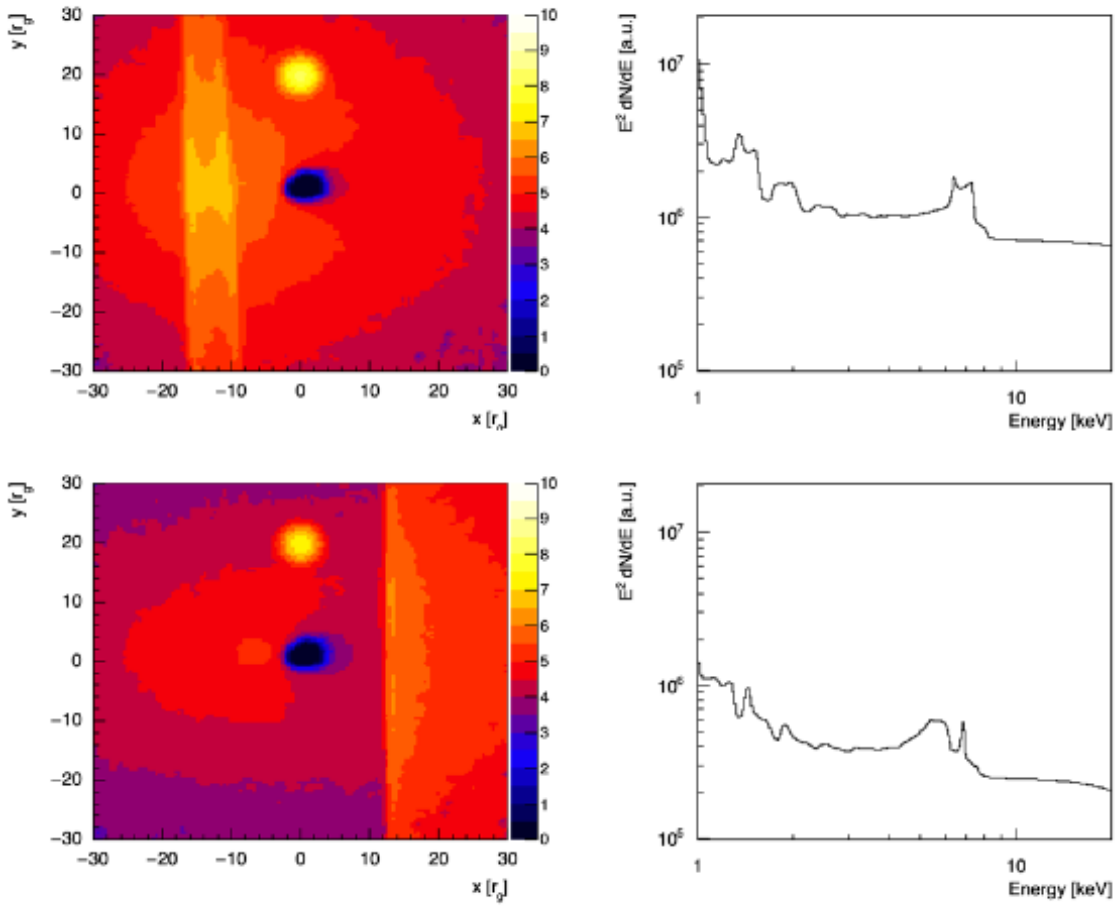

The left panels show the surface brightness of the Fe K line emission during caustic crossings over a black hole of spin a = 0.9.

The right panels show the resulting spectra of the FeKa emission in the rest frame of the source. Notice the correlated change between the FeKa line and fluorescent lines at lower energies.

(Krawczynski, Chartas and Kislat, 2019)

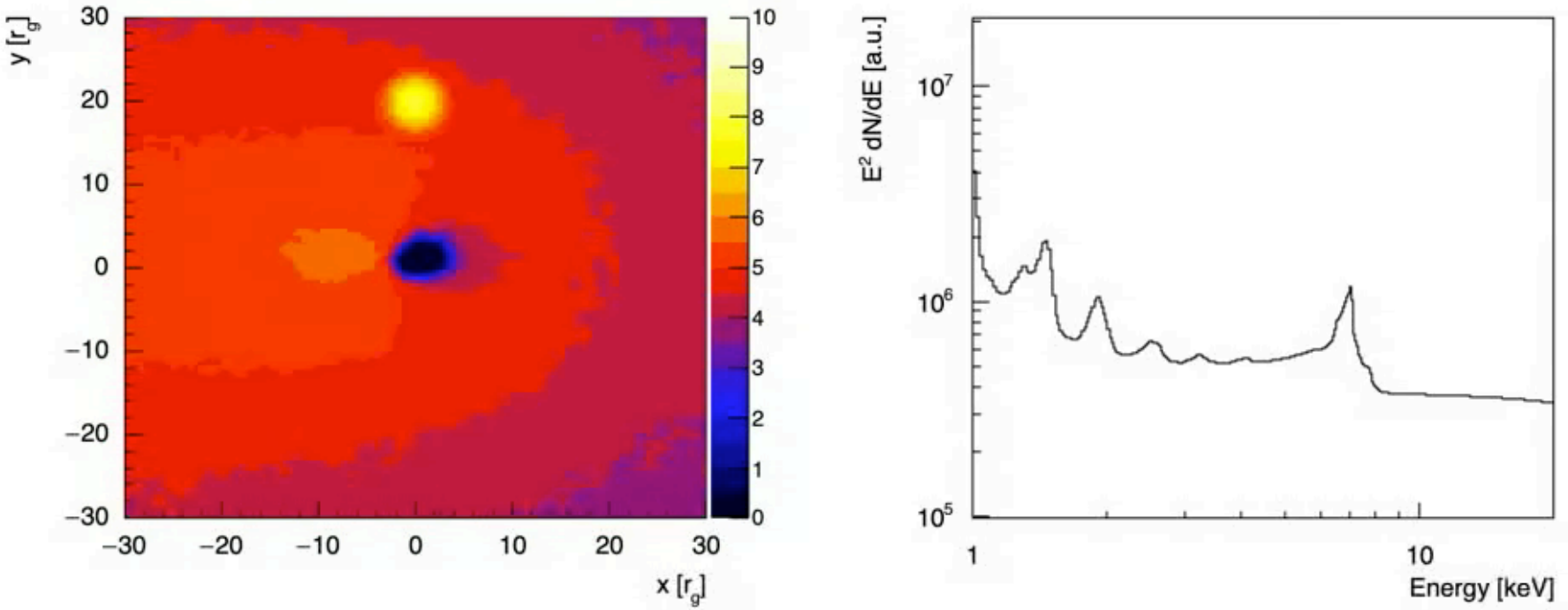

Krawczynski+ 2020

Evidence for Microlensed Fe lines in Quasar Spectra

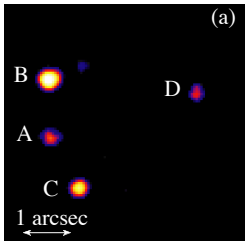

image C

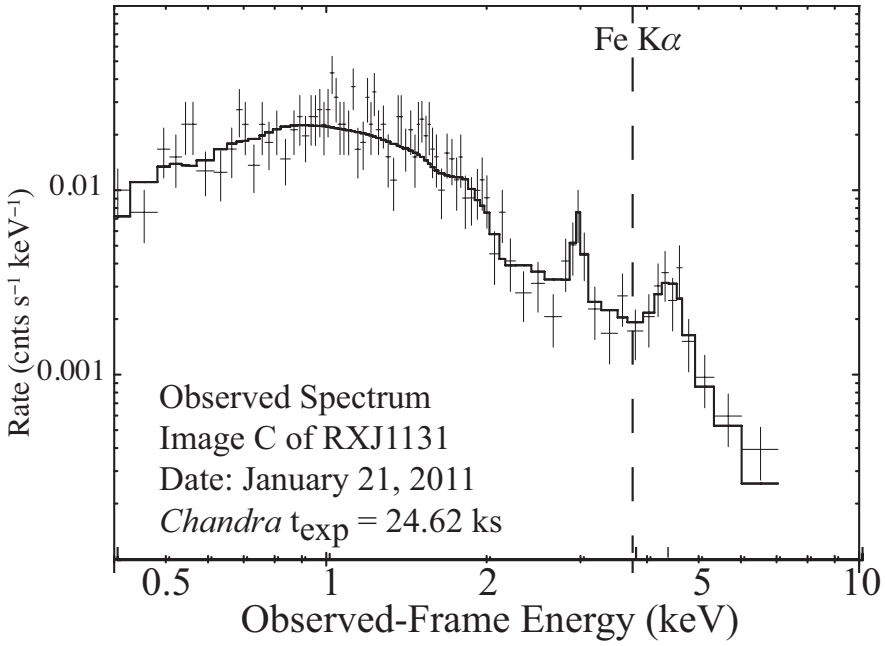

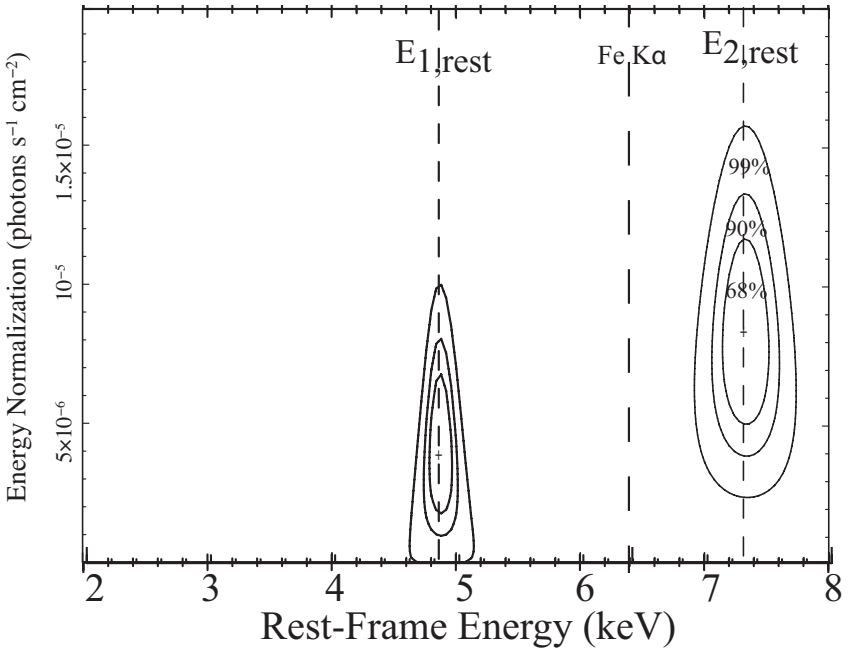

Microlesning of RX J1131-1231 in Optical and X-ray